Hyperbolicity-Preserving Stochastic Galerkin Method for Shallow Water Equations with Uncertainties

Dihan Dai,
jointly with Yekaterina Epshteyn and Akil Narayan

Department of Mathematics, University of Utah

Overview

Shallow Water Equations

Shallow Water Equations

The 2D Saint-Venant system of shallow water equations (SWE) is given by:

$$(h)_t + (q^x)_x + (q^y)_y = 0,$$
$$(q^x)_t + \left(\frac{(q^x)^2}{h} + \frac{1}{2}gh^2\right)_x + \left(\frac{q^x q^y}{h}\right)_y = -ghB_x,$$
$$(q^y)_t + \left(\frac{q^x q^y}{h}\right)_x + \left(\frac{(q^y)^2}{h} + \frac{1}{2}gh^2\right)_y = -ghB_y,$$

(1)

where

- g: the gravitational constant,
- h: the height of the water,
- q^x, q^y: the x- and y-discharges of the water, respectively,
- $B(x, y)$: bottom topography function.

It can be obtained by depth-averaging the incompressible three-dimensional Navier-Stokes equations

Shallow Water Equations: Applications

- Applications:
  - Tsunami
  - Storm surge
  - Dam break flooding
  - Landslides and avalanche
- "Shallow" means that the vertical scale of the flow is negligible compared to the horizontal scale of the flow.

Balanced/Conservation Laws

The vector form of SWE is

$$U_t + F(U)_x + G(U)_y = S(x, y, U)$$

with I.C. and B.C.

where

-
$$U = \begin{pmatrix} h \\ q^x \\ q^y \end{pmatrix}, F(U) := \begin{pmatrix} q^x \\ \frac{(q^x)^2}{h} + \frac{1}{2}gh^2 \\ \frac{q^x q^y}{h} \end{pmatrix}, G(U) := \begin{pmatrix} q^y \\ \frac{q^x q^y}{h} \\ \frac{(q^y)^2}{h} + \frac{1}{2}gh^2 \end{pmatrix},$$

- $S(x, y, U) = -gh(0, B_x, B_y)^\top$. The system is called a conservation law if $S \equiv 0$, e.g., a flat bottom, $B(x, y) = $ const.

Balanced/Conservation Laws

$$U_t + F(U)_x + G(U)_y = S(x, y, U)$$

with I.C. and B.C.

- The system is called *hyperbolic* if the eigenvalues of the matrix

$$n_x \frac{\partial F}{\partial U} + n_y \frac{\partial G}{\partial U}$$

is real-diagonalizable for any unit vector $\boldsymbol{n} = (n_x, n_y)^\top$.

- SWE is hyperbolic when $h > 0$.

Shallow Water Equations: Mathematical Difficulties

- Discontinuities can arise spontaneously in balanced/conservation laws.
  - Integral solution of a balanced law:

  $$\int_C U(x, y, t_2) \, dx \, dy = \int_C U(x, y, t_1) \, dx \, dy$$
  $$- \int_{t_1}^{t_2} \int_{\partial C} (n_x F(U) + n_y G(U)) \, ds \, dt + \int_{t_1}^{t_2} \int_C S(x, y, U) \, dx \, dy \, dt$$

  where $C \times [t_1, t_2]$ is a prescribed spatial-temporal control volume, and $\boldsymbol{n} = (n_x, n_y)^\top$ is the outer unit normal of the spatial domain C.

- No analytical solution can be found except for very simple initial conditions.

- Well-balanced property:
  - A well-balanced scheme should capture the exact solutions or small perturbations to *"lake-at-rest"* steady-state

  $$q^x = q^y \equiv 0, \quad g(h + B) \equiv \text{const}$$

  on relatively coarse grids.
  - A non-well-balanced scheme suffers numerical instability on coarse grids.
- Positivity-preserving: the height $h \geq 0$ during time evolution.
  - $h < 0$ is physically meaningless.
  - Analytically, SWE loses hyperbolicity when $h < 0$.

Numerical Solver:
Central-upwind Scheme

Central-upwind Scheme

The central-upwind scheme is a *second-order* Godunov-type finite volume scheme whose semi-discrete form is

$$\frac{d}{dt}\overline{U}_{i,j} = -\frac{\mathcal{F}_{i+\frac{1}{2},j} - \mathcal{F}_{i-\frac{1}{2},j}}{\Delta x} - \frac{\mathcal{G}_{i,j+\frac{1}{2}} - \mathcal{G}_{i,j-\frac{1}{2}}}{\Delta y} + \overline{S}_{i,j},$$

which is an approximation to the integral form of the system of the balanced law.

- $\overline{U}_{i,j} \approx \frac{1}{|C_{i,j}|} \int_{C_{i,j}} U(x, y, t) dx\, dy$.
- It is a well-developed scheme for solving hyperbolic systems of balanced/conservation laws. [Nessyahu and Tadmor, 1990, Kurganov and Tadmor, 2000, Kurganov et al., 2001, Kurganov et al., 2007, Chertock et al., 2015, Liu et al., 2018].

Central-upwind Scheme

- It is a Riemann-solver-free scheme with an upwind nature and thus computationally cheaper than the Riemann-solver-based methods.

- With modifications, structures such as the positivity and the well-balanced properties can be preserved for the discrete solution.

- At each discrete time level, the solution is approximated by a piecewise linear (conservative, second-order accurate, non-oscillatory) reconstruction.

$$\widetilde{U}(x, y) = \overline{U}_{i,j} + (U_x)_{i,j}(x - x_i) + (U_y)_{i,j}(y - y_j), \quad (x, y) \in C_{i,j}$$

- The reconstruction is then evolved to the new time level using the integral form of the balanced law.

- The semi-discrete system is solved by a stable ODE solver of an appropriate order.

Central-upwind Scheme

- In the cell $C_{i,j} = [x_{i-\frac{1}{2}}, x_{i+\frac{1}{2}}] \times [y_{j-\frac{1}{2}}, y_{j+\frac{1}{2}}]$, the approximated fluxes at the cell interfaces are given by

$$\mathcal{F}_{i+\frac{1}{2},j} := \frac{a^+_{i+\frac{1}{2},j} F(U^E_{i,j}) - a^-_{i+\frac{1}{2},j} F(U^W_{i+1,j})}{a^+_{i+\frac{1}{2},j} - a^-_{i+\frac{1}{2},j}} + \frac{a^+_{i+\frac{1}{2},j} a^-_{i+\frac{1}{2},j}}{a^+_{i+\frac{1}{2},j} - a^-_{i+\frac{1}{2},j}} \left[U^W_{i+1,j} - U^E_{i,j} \right],$$

$$\mathcal{G}_{i+\frac{1}{2},j} := \frac{b^+_{i,j+\frac{1}{2}} G(U^N_{i,j}) - b^-_{i,j+\frac{1}{2}} G(U^S_{i,j+1})}{b^+_{i,j+\frac{1}{2}} - b^-_{i,j+\frac{1}{2}}} + \frac{b^+_{i,j+\frac{1}{2}} b^-_{i,j+\frac{1}{2}}}{b^+_{i,j+\frac{1}{2}} - b^-_{i,j+\frac{1}{2}}} \left[U^S_{i,j+1} - U^N_{i,j} \right].$$

- $U^W_{i,j}, U^E_{i,j}, U^S_{i,j}, U^N_{i,j}$ are the reconstructed values of the $\widetilde{U}(x,y)$ at the cell interfaces.

-
$$\overline{S}_{i,j} \approx \frac{1}{|C_{i,j}|} \int_{C_{i,j}} S(x,y,U) dxdy,$$

is a well-balanced discretization of the source term (to cancel the numerical flux exactly in "lake-at-rest" problems).

Central-upwind Scheme

- $$a_{i+\frac{1}{2},j}^{+} = \max\left\{\lambda_N\left(\frac{\partial F}{\partial U}(U_{i+1,j}^W)\right), \lambda_N\left(\frac{\partial F}{\partial U}(U_{i,j}^E)\right), 0\right\},$$

  $$a_{i+\frac{1}{2},j}^{-} = \min\left\{\lambda_1\left(\frac{\partial F}{\partial U}(U_{i+1,j}^W)\right), \lambda_1\left(\frac{\partial F}{\partial U}(U_{i,j}^E)\right), 0\right\},$$

  $$b_{i,j+\frac{1}{2}}^{+} = \max\left\{\lambda_N\left(\frac{\partial G}{\partial U}(U_{i,j+1}^S)\right), \lambda_N\left(\frac{\partial G}{\partial U}(U_{i,j}^N)\right), 0\right\},$$

  $$b_{i,j+\frac{1}{2}}^{-} = \min\left\{\lambda_1\left(\frac{\partial G}{\partial U}(U_{i,j+1}^S)\right), \lambda_1\left(\frac{\partial G}{\partial U}(U_{i,j}^N)\right), 0\right\},$$

  are the propagation speeds at cell interfaces.

- Computing the propagation speeds is the *major* cost in solving the stochastic Galerkin formulation of shallow water equations.

12

Hyperbolicity-Preserving Stochastic Galerkin Method for Shallow Water Equations with Uncertainties

Uncertainties in Shallow Water Equations: Motivation

Due to the intrinsic uncertainties of scientific devices, the uncertainties can enter the system of the shallow water equations through

- the initial water displacements, or/and
- the bottom topography.

For example, if we model the bottom topography B as a d-dimensional random field

$$B(x, y, \xi) = B_0(x) + \sum_{k=1}^{d} B_k(x)\xi_k,$$

where $\xi = (\xi_1, \cdots, \xi_d)$ is a d-dimensional random variable,

Modelling Uncertainties in Shallow Water Equations

the stochastic bottom will lead to ξ-parametrized system of shallow water equations,

$$(h(x, y, t; \xi))_t + (q^x(x, y, t; \xi))_x + (q^y(x, y, t; \xi))_y = 0,$$

$$(q^x(x, y, t; \xi))_t + \left(\frac{(q^x(x, y, t; \xi))^2}{h(x, y, t; \xi)} + \frac{gh^2(x, y, t; \xi)}{2} \right)_x + \left(\frac{q^x(x, y, t; \xi)q^y(x, y, t; \xi)}{h(x, y, t; \xi)} \right)_y$$
$$= -gh(x, y, t; \xi)B_x(x, y; \xi),$$

$$(q^y(x, y, t; \xi))_t + \left(\frac{q^x(x, y, t; \xi)q^y(x, y, t; \xi)}{h(x, y, t; \xi)} \right)_x + \left(\frac{(q^y(x, y, t; \xi))^2}{h(x, y, t; \xi)} + \frac{gh^2(x, y, t; \xi)}{2} \right)_y$$
$$= -gh(x, y, t; \xi)B_y(x, y; \xi).$$

In order to provide more reliable model-based predictions, understanding how the uncertainties propagate in the model is necessary.

Modeling Uncertainties in Shallow Water Equations: Polynomial Chaos Expansion

- For a given second-order random field $f(\xi)$, the polynomial chaos expansion (PCE) [Xiu and Karniadakis, 2002] is the spectral expansion:

$$f(\xi) = \sum_{k=1}^{\infty} \hat{f}_k \phi_k(\xi), \qquad \phi_1(\xi) = 1.$$

where ξ is a known random variable, $\{\phi_k(\xi)\}_{k=1}^{\infty}$ are the orthonormal polynomial basis functions with respect to the density function $\rho(\xi)$ of ξ.

Modeling Uncertainties in Shallow Water Equations: Polynomial Chaos Expansion

- The *K-term PCE approximation* is the truncation in the finite-dimensional polynomial space $P_K = \text{span}\{\phi_k\}_{k\in[K]}$:

$$f(\xi) \approx f_K(\xi) = \sum_{k=1}^{K} \hat{f}_k \phi_k(\xi)$$

- K is the dimension of the solution space. The only requirement for P_K is that it contains $\phi_1 = 1$.

- Using the orthogonality, it can be shown that

$$\mathbb{E}[f_K(\xi)] = \hat{f}_1, \quad \text{var}(f_K(\xi)) = \sum_{k=2}^{K} \hat{f}_k^2$$

Modeling Uncertainties in Shallow Water Equations: Polynomial Chaos Expansion

Ansatz: the solutions are in the space $P_K = \text{span}\{\phi_k\}_{k \in [K]}$, i.e.,

$$h \simeq h_K := \sum_{k=1}^{K} \widehat{h}_k(x, y, t)\phi_k(\xi),$$

$$q^x \simeq (q^x)_K := \sum_{k=1}^{K} \widehat{(q^x)}_k(x, y, t)\phi_k(\xi),$$

$$q^y \simeq (q^y)_K := \sum_{k=1}^{K} \widehat{(q^y)}_k(x, y, t)\phi_k(\xi),$$

Stochastic Galerkin Method

One way to solve the truncated PCE system is the stochastic Galerkin method, which seeks a solution in the solution space P_K such that the residual is orthogonal to P_K.

- Stochastic Galerkin (SG) method leads to a new system of PDEs for the coefficients of polynomials in the K-term PCE approximation. SG method is intrusive since it requires new solvers and new codes for the new system.

- There are many provable properties for SG systems. For example, it is near optimal in L_ρ^2 sense for the stationary problems.

- It is a well-established method for diffusion-dominated and stationary problems
  [Xiu and Shen, 2009, Cohen et al., 2010, Ullmann et al., 2012].

- It is less mature and settled for hyperbolic system of conservation/balanced laws.

Stochastic Galerkin Method: Challenges Ahead

- Hyperbolicity-Preserving:
    - SG systems may loss hyperbolicity [Després et al., 2013].
    - In [Wu et al., 2017], a strategy is proposed to regain the hyperbolicity of the quasilinear hyperbolic system, but it is limited to the quasilinear form.
    - In [Gerster et al., 2019], the PCEs of the Roe variables are introduced. But the approach is effective for certain choices of distributions for ξ.
    - In [Poëtte et al., 2009], the PCEs of the entropy variables are introduced. But the approach requires to solve an optimization problem for every cell at every time step. The computations can be very expensive.

Stochastic Galerkin Method: Challenges Ahead

- Well-Balanced Preserving:
  - The numerical solution should preserve the stochastic variant of the "lake-at-rest" solution

$$q_K^x(x, y, t; \xi) = q_K^y(x, y, t; \xi) \equiv 0,$$
$$h_K(x, y, t; \xi) + \mathcal{G}_K[B](x, y; \xi) \equiv C(\xi).$$

- Our contributions [Dai et al., 2021]
  - We derive a hyperbolicity-preserving stochastic Galerkin formulations using only the PCEs of the conserved variables (h, q^x, q^y) and a stochastic variant $\mathcal{P}(\hat{h}) > 0$ of the deterministic positivity condition to guarantee the hyperbolicity.
  - We develop a central-upwind type scheme that can preserve stochastic positivity condition $\mathcal{P}(\hat{h}) > 0$ and thus preserve hyperbolicity at discrete time levels.
  - We derive a well-balanced discretization of the source term for our scheme.
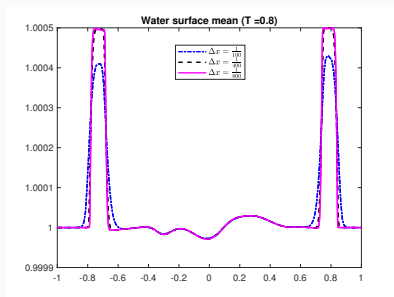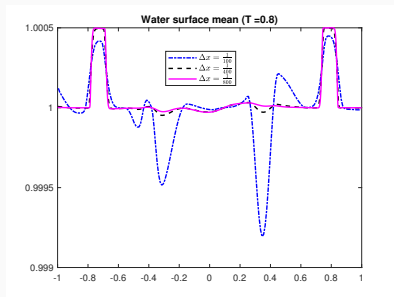
Figure 1: Instability in a non-well-balanced scheme. Left: numerical results of a non-well-balanced scheme. Right: numerical results of a well-balanced scheme

For a 2nd-order random field $z(\xi)$, define the K-term PCE operator $\mathcal{G}_K$ to be

$$\mathcal{G}_K[z](\xi) := \sum_{k=1}^{K} \widehat{z}_k \phi_k(\xi)$$

Denote the vector of the coefficients in by

$$\widehat{z} = (\widehat{z}_1, \cdots, \widehat{z}_K)^\top.$$

Preliminaries: PCE for Product And Ratio

The K-term PCE for the product of two random fields $a(\xi)$ and $b(\xi)$ is usually approximated by their *pseudo-spectral product*

$$\mathcal{G}_K[a, b] := \mathcal{G}_K\left[\mathcal{G}_K[a]\,\mathcal{G}_K[b]\right] = \sum_{k=1}^{K}\left(\sum_{m,\ell=1}^{K}\widehat{a}_m\widehat{b}_\ell\langle\phi_m\phi_\ell, \phi_k\rangle_\rho\right)\phi_k(\xi).$$

For single-signed radom field $a(\xi)$, the K-term PCE of ratio b/a can be approximated by solving

$$\mathcal{G}_K\left[a, \frac{b}{a}\right] = \mathcal{G}_K[b]$$

Preliminaries: PCE for Product And Ratio

Define the symmetric matrix:

$$\mathcal{P}(\widehat{a}) := \sum_{k=1}^{K} \widehat{a}_k \mathcal{M}_k \qquad \mathcal{M}_k := (\langle \phi_\ell \phi_m, \phi_k \rangle_\rho)_{\ell,m=0,\cdots,K}$$

Then the PCE of the pesudo-spectral product is

$$\widehat{\mathcal{G}_K[a,b]} = \mathcal{P}(\widehat{a})\widehat{b} = \mathcal{P}(\widehat{b})\widehat{a},$$

and the PCE of the ratio is the solution to

$$\mathcal{P}(\widehat{a})\widehat{\left(\frac{b}{a}\right)} = \widehat{b},$$

whose solution introduce a new operator

$$\mathcal{G}_K^{\dagger}\left[\frac{b}{a}\right](\xi) := \sum_{k=1}^{K} c_k \phi_k(\xi),$$

Assumptions for Hyperbolicity-Preserving Formulation

- For $(q^x)^2/h$ and $(q^y)^2/h$ terms:

$$\frac{(q^x)^2}{h} = q^x \frac{q^x}{h}; \quad \longrightarrow \quad \mathcal{G}_K \left[\frac{(q_K^x)^2}{h_K} \right] = \mathcal{G}_K \left[q_K^x \, \mathcal{G}_K^\dagger \left[\frac{q_K^x}{h_K} \right] \right],$$

$$\frac{(q^y)^2}{h} = q^y \frac{q^y}{h} \quad \longrightarrow \quad \mathcal{G}_K \left[\frac{(q_K^y)^2}{h_K} \right] = \mathcal{G}_K \left[q_K^y \, \mathcal{G}_K^\dagger \left[\frac{q_K^y}{h_K} \right] \right].$$

- For $q^x q^y / h$ terms

$$\frac{q^x q^y}{h} = q^x \frac{q^y}{h} \quad \longrightarrow \quad \mathcal{G}_K \left[\frac{q_K^x q_K^y}{h_K} \right] = \mathcal{G}_K \left[q_K^x \, \mathcal{G}_K^\dagger \left[\frac{q_K^y}{h_K} \right] \right] \quad \text{in } x\text{-direction,}$$

$$\frac{q^x q^y}{h} = q^y \frac{q^x}{h} \quad \longrightarrow \quad \mathcal{G}_K \left[\frac{q_K^x q_K^y}{h_K} \right] = \mathcal{G}_K \left[q_K^y \, \mathcal{G}_K^\dagger \left[\frac{q_K^x}{h_K} \right] \right] \quad \text{in } y\text{-direction.}$$

Note that, in general, the two approximations for $q^x q^y / h$ are different.

With these assumptions, we obtain

$$
\underbrace{\begin{pmatrix} \widehat{h} \\ \widehat{q^x} \\ \widehat{q^y} \end{pmatrix}_t}_{\widehat{U}_t} + \underbrace{\begin{pmatrix} \widehat{q^x} \\ \mathcal{P}(\widehat{q^x})\mathcal{P}^{-1}(\widehat{h})\widehat{q^x} + \frac{1}{2}g\mathcal{P}(\widehat{h})\widehat{h} \\ \mathcal{P}(\widehat{q^x})\mathcal{P}^{-1}(\widehat{h})\widehat{q^y} \end{pmatrix}_x}_{F(\widehat{U})_x} + \underbrace{\begin{pmatrix} \widehat{q^y} \\ \mathcal{P}(\widehat{q^y})\mathcal{P}^{-1}(\widehat{h})\widehat{q^x} \\ \mathcal{P}(\widehat{q^y})\mathcal{P}^{-1}(\widehat{h})\widehat{q^y} + \frac{1}{2}g\mathcal{P}(\widehat{h})\widehat{h} \end{pmatrix}_y}_{G(\widehat{U})_y}
$$
$$
= \underbrace{\begin{pmatrix} 0 \\ -g\mathcal{P}(\widehat{h})\widehat{B_x} \\ -g\mathcal{P}(\widehat{h})\widehat{B_y} \end{pmatrix}}_{S(\widehat{U},\widehat{B})}.
$$

(2)

Hyperbolicity-Preserving SG Formulation

Theorem 1.

If the matrix $\mathcal{P}(\widehat{h})$ is strictly positive definite, the SG formulation (2) is hyperbolic.

- In general, the theorem does not hold for other stochastic Galerkin formulations of the shallow water equations.

- The condition $\mathcal{P}(\widehat{h}) > 0$ is a stochastic variant of the positive water height. When there is no uncertainty, it reduces to the hyperbolicity condition $h > 0$ for the deterministic shallow water equations,

$$\mathcal{P}(\widehat{h}) = (\widehat{h}_1)\mathsf{Id} > 0 \Leftrightarrow \widehat{h}_1 > 0.$$

Hyperbolicity-Preserving SG Formulation

Theorem 2.

Given K, let nodes ξ_m and weights τ_m satisfying $\{(\xi_m, \tau_m)\}_{m=1}^{M} \subset \mathbb{R}^d \times (0, \infty)$ represent any M-point positive quadrature rule that is exact on P_K^3, i.e.,

$$\int_{\mathbb{R}^d} p(\xi)\rho(\xi)d\xi = \sum_{m=1}^{M} p(\xi_m)\tau_m, \qquad p \in P_K^3,$$

where P_K^3 is the set of all the triple products of the elements in P_K. If

$$h_K(x, y, t; \xi_m) > 0 \ \forall \ m = 1, \ldots, M,$$

then the stochastic Galerkin system (2) *is hyperbolic.*

Summary of Our Scheme

- We derive a CFL-type condition to preserve the hyperbolicity of our SG system at every discrete time level for the cell averages.

- We introduce a filter to preserve the hyperbolicity of the system at the cell interfaces in the second-order piecewise linear reconstructions,

$$\widetilde{U}(x,y) = \overline{U}_{i,j} + (\widehat{U}_x)_{i,j}(x - x_i) + (\widehat{U}_y)_{i,j}(y - y_j), \quad (x,y) \in C_{i,j}.$$

- We introduce other reconstruction procedures to tackle the possible failures of the code at near dry state ($h \sim 0$) due to round-off errors.

- We derive a well-balanced discretization of the source term that captures the stochastic "lake-at-rest" state exactly at discrete level.

Hyperbolicity-Preserving Time Discretization

Lemma 3.

Let $\{\xi_m\}_{m \in [M]}$ be the nodes of a quadrature rule satisfying the conditions of theorem 2 and $\Phi(\xi) = (\phi_1(\xi), \ldots, \phi_K(\xi))^\top$. Denote the numerical approximation to $\overline{\tilde{h}}_{i,j}(t^n)$ by $\overline{\tilde{h}}_{i,j}^n$ and $\Delta t_n := t^{n+1} - t^n$. Assume that $\overline{\tilde{h}}_{i,j}^n(\xi_m) := (\overline{\tilde{h}}_{i,j}^n)^\top \Phi(\xi_m) > 0$ for $m \in [M]$. If Δt^n satisfies

$$\Delta t^n < \Delta t_h^n := \min_{\substack{m \in [M] \\ i \in [N_x], j \in [N_y]}} \left\{ \left| \left| \frac{(\overline{\tilde{h}}_{i,j}^n)^\top \Phi(\xi_m)}{\left[\frac{\mathcal{F}_{i+\frac{1}{2},j}^{\hat{h}}(t_n) - \mathcal{F}_{i-\frac{1}{2},j}^{\hat{h}}(t_n)}{\Delta x} + \frac{\mathcal{G}_{i,j+\frac{1}{2}}^{\hat{h}}(t_n) - \mathcal{G}_{i,j-\frac{1}{2}}^{\hat{h}}(t_n)}{\Delta y} \right]^\top \Phi(\xi_m)} \right| \right| \right\},$$

then the flux Jacobian is diagonalizable with real eigenvalues at the cell averages $\overline{\hat{U}}_{i,j}$.

Filtering at Pointwise Reconstructions

We filter $\widehat{h}_{i,j}^{W,E,N,S}$ by

$$\left(\widehat{\boldsymbol{h}}_{i,j}^{W,E,N,S}\right)_1 = \left(\widehat{h}_{i,j}^{W,E,N,S}\right)_1,$$
$$\left(\widehat{\boldsymbol{h}}_{i,j}^{W,E,N,S}\right)_k = (1 - \mu_{i,j}^n)\left(\widehat{h}_{i,j}^{W,E,N,S}\right)_k, k = 2, \ldots, K, \tag{3}$$

where $\mu_{i,j}^n$ is a parameter such that

$$\boldsymbol{h}_{i,j}^{W,E,N,S}(\xi_m) = (1 - \mu_{i,j}^n)(\widehat{h}_{i,j}^{W,E,N,S})_1 + \mu_{i,j}^n h_{i,j}^{W,E,N,S}(\xi_m) > 0$$

for all quadrature points $\xi_m, m \in [M]$.

Reconstructing Negative First Moment

For negative first moment, instead of using filter, we use the reconstruction,

$$\text{if } \left(\widehat{h}_{i,j}^{W}\right)_1 \le 0 \text{ then take } \widehat{h}_{i,j}^{W} = 0, \ \ \widehat{h}_{i,j}^{E} = 2\overline{\widehat{h}}_{i,j}^{n},$$

$$\text{if } \left(\widehat{h}_{i,j}^{E}\right)_1 \le 0 \text{ then take } \widehat{h}_{i,j}^{E} = 0, \ \ \widehat{h}_{i,j}^{W} = 2\overline{\widehat{h}}_{i,j}^{n},$$

$$\text{if } \left(\widehat{h}_{i,j}^{N}\right)_1 \le 0 \text{ then take } \widehat{h}_{i,j}^{N} = 0, \ \ \widehat{h}_{i,j}^{S} = 2\overline{\widehat{h}}_{i,j}^{n},$$

$$\text{if } \left(\widehat{h}_{i,j}^{S}\right)_1 \le 0 \text{ then take } \widehat{h}_{i,j}^{N} = 0, \ \ \widehat{h}_{i,j}^{N} = 2\overline{\widehat{h}}_{i,j}^{n}.$$

Velocity Desingularization

In the central-upwind scheme, we need to compute the PCE for the velocities

$$\widehat{u} = \mathcal{P}^{-1}(\widehat{h})\widehat{q}^x, \qquad\qquad \widehat{v} = \mathcal{P}^{-1}(\widehat{h})\widehat{q}^y,$$

which may produce large roundoff error when $\mathcal{P}(\widehat{h})$ is near singular.

Velocity Desingularization

We proposed the following desingularization process

$$\widehat{u} = \mathcal{P}_{\text{cor}}^{-1}(\widehat{h})\widehat{q}^x, \qquad\qquad \widehat{v} = \mathcal{P}_{\text{cor}}^{-1}Q\widehat{q}^y, \qquad\qquad (4)$$

where

$$\mathcal{P}_{\text{cor}}^{-1}(\widehat{h}) = Q^\top \Pi_{\text{cor}} Q.$$

Here, Q is the eigenmatrix such that $\mathcal{P}^{-1}(\widehat{h}) = Q^\top \Pi Q$,
$\Pi = \text{diag}(\lambda_1, \ldots, \lambda_K)$ is the diagonal matrix of eigenvalues, and

$$\Pi^{\text{cor}} = \text{diag}(\lambda_1^{\text{cor}}, \ldots, \lambda_K^{\text{cor}}), \qquad \lambda_k^{\text{cor}} = \frac{\sqrt{2}\lambda_k}{\sqrt{\lambda_k^4 + \max\{\lambda_k^4, \epsilon^4\}}}.$$

.

Well-Balanced Property

A stochastic variant of the well-balanced property is

$$q_K^x(x, y, t; \xi) = q_K^y(x, y, t; \xi) \equiv 0, \quad h_K(x, y, t; \xi) + \mathcal{G}_K[B](x, y; \xi) \equiv C(\xi),$$

which is equivalent to

$$\widehat{q^x} = \widehat{q^y} \equiv 0, \quad \widehat{h} + \widehat{B} \equiv \widehat{C}.$$

Well-Balanced Property

Theorem 4.
The central-upwind scheme is well-balanced if we choose
$$\overline{\overline{\widehat{S}}}_{ij} = \left((\overline{\overline{\widehat{S}}}_{i,j}^{(1)})^{\top}, (\overline{\overline{\widehat{S}}}_{i,j}^{(2)})^{\top}, (\overline{\overline{\widehat{S}}}_{i,j}^{(3)})^{\top} \right)^{\top}, \text{ where}$$

$$\begin{cases}
\overline{\overline{\widehat{S}}}_{i,j}^{(1)} = 0, \\
\overline{\overline{\widehat{S}}}_{i,j}^{(2)} = -g\mathcal{P}(\overline{\overline{h}}_{i,j})\left(\dfrac{\widehat{B}_{i+\frac{1}{2},j} - \widehat{B}_{i-\frac{1}{2},j}}{\Delta x} \right), \\
\overline{\overline{\widehat{S}}}_{i,j}^{(3)} = -g\mathcal{P}(\overline{\overline{h}}_{i,j})\left(\dfrac{\widehat{B}_{i,j+\frac{1}{2}} - \widehat{B}_{i,j-\frac{1}{2}}}{\Delta y} \right).
\end{cases}$$

Numerical Results

Numerical Example: Comparison with Collocation Solution

A deterministic water surface

$$w(x, 0; \xi) = \begin{cases} 1 & x < 0 \\ 0.5 & x > 0 \end{cases}, \quad q(x, 0; \xi) = 0, \tag{5}$$

and with a stochastic bottom topography

$$B(x; \xi) = \begin{cases} 0.125(\cos(5\pi x) + 2) + 0.125\xi, & |x| < 0.2 \\ 0.125 + 0.125\xi, & \text{otherwise} \end{cases}, \tag{6}$$

where $\xi \sim \mathcal{U}(-1, 1)$.
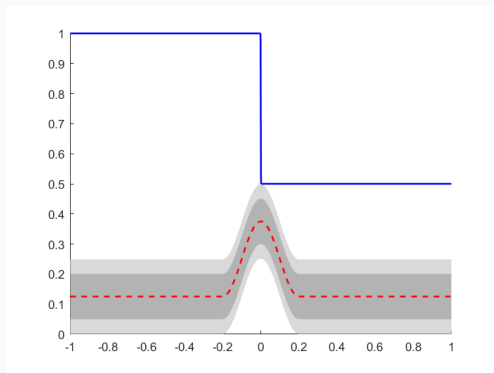
Figure 2: Initial Water Surface for Equation (5)-Equation (6). Blue solid line: water surface. Red dashed line: mean bottom topography. Light grey region: the $0.005 - 0.995$ quantile of the stochastic bottom. Dark grey region: the $0.2 - 0.8$ quantile of the stochastic bottom.

Figure 3: Results for Equation (5)-Equation (6), water surfaces. Top left: stochastic Galerkin, $K = 9, \Delta x = 1/800$. Top right: stochastic Galerkin, $K = 17, \Delta x = 1/800$. Bottom: stochastic collocation, $K = 9, \Delta x = 1/800$. Pink dot-dashed line: variance of the water surface.

Numerical Example: Comparison with Collocation Solution
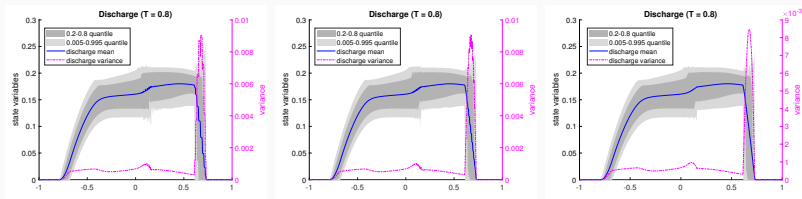
Figure 4: Results for Equation (5)-Equation (6), discharges. Top left: stochastic Galerkin, $K = 9, \Delta x = 1/800$. Top right: stochastic Galerkin, $K = 17, \Delta x = 1/800$. Bottom: stochastic collocation, $K = 9, \Delta x = 1/800$. Pink dot-dashed line: variance of the discharges.

Numerical Example: Possible Loss of Positivity

Another deterministic water surface

$$w(x, 0; \xi) = \begin{cases} 5.0 & x \leq 0.5, \\ 1.6 & x > 0.5, \end{cases} \qquad u(x, 0, \xi) = \begin{cases} 1.0 & x \leq 0.5, \\ -2.0 & x > 0.5, \end{cases} \tag{7}$$

and a stochastic discontinuous bottom

$$B(x; \xi) = \begin{cases} 1.5 + 0.1\xi & x \leq 0.5, \\ 1.1 + 0.1\xi & x > 0.5, \end{cases} \tag{8}$$

where $\xi \sim \text{Beta}(2, 4)$.

Numerical Example: Possible Loss of Positivity
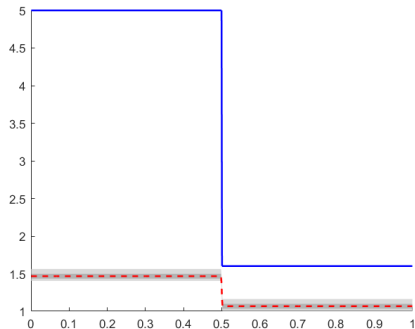
Figure 5: Initial Water Surface for Equation (7)-Equation (8). Blue solid line: water surface. Red dashed line: mean bottom topography. Light grey region: the $0.005 - 0.995$ quantile of the stochastic bottom. Dark grey region: the $0.2 - 0.8$ quantile of the stochastic bottom.

Numerical Example: Possible Loss of Positivity

M	$\max_m \xi_m$	Negative Region N_M	$\Pr[\xi \in N_M]$
15	0.934077	[0.934079, 1]	5.75×10^{-6}
17	0.946839	[0.946899, 1]	2.43×10^{-6}
19	0.956205	[0.956320, 1]	1.12×10^{-6}
21	0.963310	[0.963980, 1]	5.18×10^{-7}

Table 1: Numerical study of ξ-region and associated probabilities where the water height is negative.

Increasing the number of quadrature points will make the negative water height less likely to occur.

Numerical Example: Order of Convergence

$$w(x, y, 0; \xi) = 1, \quad u(x, y, 0; \xi) = 0.3, \quad v(x, y, 0; \xi) = 0, \qquad (9)$$

and bottom topography:

$$B(x, y; \xi) = 0.5e^{-25(x-1)^2 - 50(y-0.5)^2} + 0.1(\xi + 1), \qquad (10)$$

where $\xi \sim \mathcal{U}(-1, 1)$.

Numerical Example: Order of Convergence
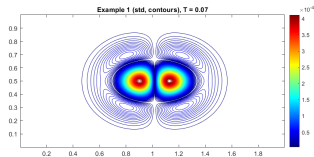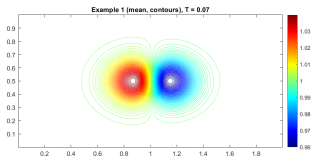
Figure 6: Reference solution (grid size 800×800) for the water Surface for Equation (9)-Equation (10) at $t = 0.07$. Left: mean. Right: standard deviation.

Numerical Example: Order of Convergence

	N=4		N=8	
	Error	Order	Error	Order
100×100	1.475875e-05	–	1.475865e-05	–
200×200	4.343711e-06	1.764571	4.343714e-06	1.764559
400×400	1.296122e-06	1.744727	1.296122e-06	1.744727

The error is computed by

$$\|u_h - u_{\text{ref}}\|_{L^1(\Omega_{x,y}), L^2(\Omega_\xi)},$$

where u_h is the numerical solution, u_{ref} is the reference solution computed on the 800×800 grid, $\Omega_{x,y}$ is the physical domain, and Ω_ξ is the stochastic domain. The orders are similar to the results in the deterministic test [Bryson et al., 2011]. We expect computing the reference solution on a finer grid will gives higher orders.

46

Numerical Example: Another Comparison with Collocation Solution

Another stochastic bottom

$$w(x,y,0;\xi) = \begin{cases} 1.01, & \text{if } 0.05 < x < 0.15, \\ 1, & \text{otherwise}, \end{cases} \qquad u(x,y,0;\xi) = v(x,y,0;\xi) = 0. \tag{11}$$

Bottom topography:

$$B(x,y;\xi) = 0.8e^{-5(x-0.9)^2 - 50(y-0.5)^2} + 0.1(\xi+1). \tag{12}$$

Numerical Example: Another Comparison with Collocation Solution
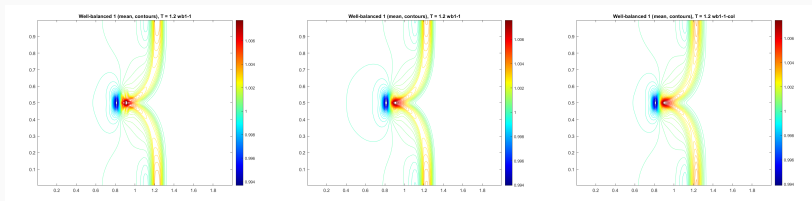
Figure 7: Numerical solutions to (11)-(12), mean water surface at $t = 1.2$, grid size 400×400. Left: $K = 4$; Middle: $K = 8$. Right: collocation solution. (60 contours). The number of collocation points is 100

Numerical Example: Another Comparison with Collocation Solution
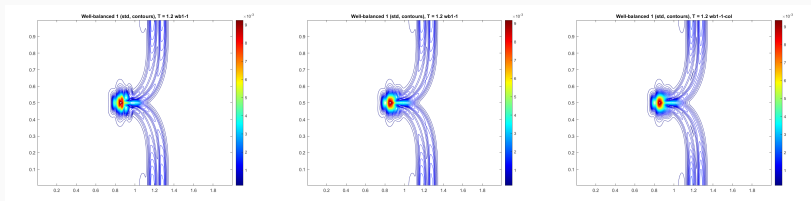
Figure 8: Numerical solutions to (11)-(12), std of the water surface at $t = 1.2$, grid size 400×400. Left: $K = 4$; Middle: $K = 8$. Right: collocation solution. (60 contours). The number of collocation points is 100

Numerical Example: Two Dimensional Stochastic Space

Uncertainties on the position of the bottom topography:

$$w(x, y, 0; \xi) = \begin{cases} 1.01, & \text{if } 0.05 < x < 0.15, \\ 1, & \text{otherwise}, \end{cases} \qquad u(x, y, 0; \xi) = v(x, y, 0; \xi) = 0.$$

(13)

Bottom topography:

$$B(x, y; \xi) = 0.8 e^{-5(x-0.9+0.1\xi_1)^2 - 50(y-0.5+0.1\xi_2)^2}. \tag{14}$$

where $\xi = (\xi_1, \xi_2)$, $\xi_1 \sim \mathcal{B}(4, 2)$, and $\xi_2 \sim \mathcal{U}(-1, 1)$. The polynomial basis are the tensorial orthonormal polynomials of degree at most 3 for ξ_1 and ξ_2.
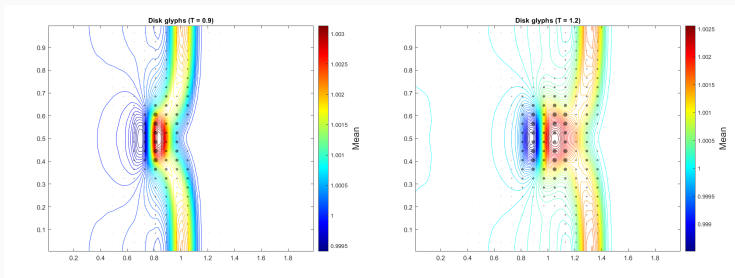
Figure 9: Numerical solution to (13)-(14), disk-glyph over mean contours, where the radii of the disks indicate the magnitude of the standard deviation, $t = 0.9, 1.2$ (left and right). The largest disks are corresponding to the standard deviation values $0.0015012, 0.0010295$, respectively.

Numerical Example: Water Around An Island

Stochastic water surface and deterministic bottom:

$$w(x, y, 0; \xi) = \begin{cases} 1 + 0.0001(\xi + 1) & \text{if } -0.4 < x < -0.3 \\ 1 & \text{otherwise} \end{cases}, \qquad (15)$$

$$u(x, y, 0; \xi) = v(x, y, 0; \xi) = 0. \qquad (16)$$

Bottom topography:

$$B(x, y; \xi) = \begin{cases} 0.9998, & r \le 0.1, \\ 9.998(0.2 - r), & 0.1 < r \le 0.2, \\ 0, & \text{otherwise}, \end{cases} \quad r := \sqrt{x^2 + y^2}. \quad (17)$$

Numerical Example: Water Around An Island
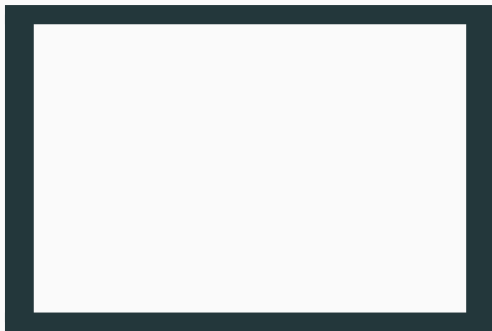
The radius of the glyphs are proportional to the values of the standard deviation at the cells. The glyphs for part of the cells are shown in the movie.

Thank you!

References

Bryson, S., Epshteyn, Y., Kurganov, A., and Petrova, G. (2011).
Well-balanced positivity preserving central-upwind scheme on triangular grids for the saint-venant system.
ESAIM: Mathematical Modelling and Numerical Analysis, 45(3):423–446.

Chertock, A., Cui, S., Kurganov, A., and Wu, T. (2015).
Well-balanced positivity preserving central-upwind scheme for the shallow water system with friction terms.
International Journal for numerical methods in fluids, 78(6):355–383.

Cohen, A., DeVore, R., and Schwab, C. (2010).
Convergence Rates of Best N-term Galerkin Approximations for a Class of Elliptic sPDEs.
Foundations of Computational Mathematics, 10(6):615–646.

References

Dai, D., Epshteyn, Y., and Narayan, A. (2021).
Hyperbolicity-preserving and well-balanced stochastic galerkin method for shallow water equations.
SIAM Journal on Scientific Computing, 43(2):A929–A952.

Després, B., Poëtte, G., and Lucor, D. (2013).
Robust uncertainty propagation in systems of conservation laws with the entropy closure method.
In *Uncertainty quantification in computational fluid dynamics*, pages 105–149. Springer.

Gerster, S., Herty, M., and Sikstel, A. (2019).
Hyperbolic stochastic galerkin formulation for the p-system.
Journal of Computational Physics.

References

Kurganov, A., Noelle, S., and Petrova, G. (2001).
Semidiscrete central-upwind schemes for hyperbolic conservation laws and hamilton–jacobi equations.
SIAM Journal on Scientific Computing, 23(3):707–740.

Kurganov, A., Petrova, G., et al. (2007).
A second-order well-balanced positivity preserving central-upwind scheme for the saint-venant system.
Communications in Mathematical Sciences, 5(1):133–160.

Kurganov, A. and Tadmor, E. (2000).
New high-resolution central schemes for nonlinear conservation laws and convection–diffusion equations.
Journal of Computational Physics, 160(1):241–282.

References

Liu, X., Albright, J., Epshteyn, Y., and Kurganov, A. (2018).
**Well-balanced positivity preserving central-upwind scheme
with a novel wet/dry reconstruction on triangular grids for the
saint-venant system.**
Journal of Computational Physics, 374:213–236.

Nessyahu, H. and Tadmor, E. (1990).
**Non-oscillatory central differencing for hyperbolic conservation
laws.**
Journal of computational physics, 87(2):408–463.

Poëtte, G., Després, B., and Lucor, D. (2009).
Uncertainty quantification for systems of conservation laws.
Journal of Computational Physics, 228(7):2443–2467.

References

📄 Ullmann, E., Elman, H. C., and Ernst, O. G. (2012).
Efficient iterative solvers for stochastic galerkin discretizations of log-transformed random diffusion problems.
SIAM Journal on Scientific Computing, 34(2):A659–A682.

📄 Wu, K., Tang, H., and Xiu, D. (2017).
A stochastic galerkin method for first-order quasilinear hyperbolic systems with uncertainty.
Journal of Computational Physics, 345:224–244.

📄 Xiu, D. and Karniadakis, G. E. (2002).
The wiener–askey polynomial chaos for stochastic differential equations.
SIAM journal on scientific computing, 24(2):619–644.

References

Xiu, D. and Shen, J. (2009).
Efficient stochastic galerkin methods for random diffusion equations.
Journal of Computational Physics, 228(2):266–281.